Search for damage and/or disordering effects due to intense electronic excitation in crystalline metallic alloys irradiated by high-energy heavy ions

1990 J. Phys.: Condens. Matter 2 1733

(http://iopscience.iop.org/0953-8984/2/7/005)

J. Phys.: Condens. Matter **2** (1990) 1733–1741. Printed in the UK

Search for damage and/or disordering effects due to intense electronic excitation in crystalline metallic alloys irradiated by high-energy heavy ions

A Dunlop†, D Lesueur†, N Lorenzelli†, A Audouard‡§, C Dimitrov‖, J M Ramillon¶ and L Thomé††

† Laboratoire des Solides Irradiés, Ecole Polytechnique, 91128 Palaiseau Cédex, France
‡ Laboratoire de Physique du Solide, BP 239, 54506 Vandoeuvre Les Nancy Cédex, France
‖ Centre d'Etudes de Chimie Métallurgique, 15 rue Georges Urbain, 94407 Vitry sur Seine Cédex, France
¶ Centre Interdisciplinaire de Recherche avec les Ions Lourds, BP 5133, 14040 Caen Cédex, France
†† Centre de Spectrométrie Nucléaire et de Spectrométrie de Masse, Bâtiment 108, 91405 Orsay Cédex, France

Received 26 June 1989, in final form 13 October 1989

Abstract. The effects of intense electronic excitation produced during high-energy heavy-ion irradiation on the damage creation processes in crystalline metallic alloys are studied by *in situ* liquid-helium electrical resistance experiments. Targets consist of stacks of austenitic Fe–Cr–Ni and both ordered and disordered Cu_3Au and Ni_3Fe piled up along the 3.4 GeV Xe beam direction in order to vary the amount of electronic energy loss inside the samples. Additional dimensional measurements performed in the case of austenitic Fe–Cr–Ni indicate no change in the sample length within the experimental uncertainty ($\Delta l/l = 10^{-3}$).

It is shown that inelastic collisions have no measurable effects on damage production in ordered or disordered Cu_3Au, while they induce a decrease in the defect production efficiency in the case of Ni_3Fe and austenitic Fe–Cr–Ni. The latter effect can be attributed to partial recombination of close Frenkel pairs induced in nuclear collisions, as already observed in pure Fe and Ni.

1. Introduction

Why should one search for damage or disordering effects by very intense electronic excitations in ordered crystalline metallic alloys, and how can this be done?

It was clearly shown in [1, 2] that, during low-temperature irradiations of amorphous metallic alloys with very-high-energy ions (from 1.76 GeV argon to 3 GeV xenon), a threshold value of the ion electronic stopping power (about 1.5 keV $Å^{-1}$) exists above which the defect production rate increases dramatically; to the usual damage due to nuclear elastic collisions, one has to add an important contribution related to electronic excitation. A study of the annealing curves has shown that the damage induced by

§ Present address: Laboratoire de Physique des Solides et Service des Champs Magnétiques Intenses, Institut National des Sciences Appliquées, Université Paul Sabatier, 31077 Toulouse, France.

0953-8984/90/071733 + 09 $03.50

electronic excitation is similar to that originating from elastic collisions with low-energy ions or electrons. Moreover, at high irradiation fluences, a strong radiation-induced growth of amorphous samples was observed [1–3]. The detailed interpretation of this phenomenon is still under discussion.

Although the mechanism of defect creation via electronic processes is not yet well understood in amorphous alloys, it seemed quite interesting to examine whether these effects are specifically connected to the nature of the arrangement of the atoms in amorphous materials or whether they also exist in crystalline metallic materials. To check this point we have studied crystalline metallic alloys having a wide range of electronic properties, Cu_3Au, Ni_3Fe and austenitic Fe–Cr–Ni, for the following reasons:

(i) Defect creation during low-temperature irradiation with electrons, neutrons and low-energy ions [4–9] has already been studied in these materials.

(ii) Cu_3Au [10] and Ni_3Fe [11] can be obtained in long-range ordered and disordered states.

(iii) Short-range ordered Fe–Cr–Ni crystalline alloys are characterised, similarly to amorphous alloys, by high electrical resistivity values and by a weak temperature dependence of the resistivity between room temperature and liquid-helium temperature (similar electrical properties in amorphous and crystalline alloys suggest similar electronic thermal conductivities in the two types of material).

(iv) All these alloys can be cold rolled down to thicknesses of a few micrometres.

The damage creation processes were investigated at liquid-helium temperature during irradiation with 3.4 GeV xenon ions which are mainly slowed down by interactions with the target electrons. Damage and chemical disordering effects were studied *in situ* via electrical resistance measurements. The lengths of some of the samples were also measured at room temperature before and after irradiation in order to demonstrate a possible growth effect.

2. Experimental procedure and damage calculation

2.1. Sample preparation

2.1.1. Cu_3Au alloys. Cu_3Au ribbons (width, about 1.5 mm; length, about 12 mm; thickness, 11 μm) were cold rolled to the desired thickness, annealed at 1070 K for 20 h in a helium atmosphere to remove the dislocations and other defects and then either

(i) annealed at temperatures slowly decreasing from 670 to 570 K in a helium atmosphere for 200 h and then cooled (steady temperature decrease for 2 d) to room temperature in order to obtain long-range-ordered alloys or

(ii) quenched (at about 10 K s^{-1}) to room temperature in order to obtain disordered alloys.

2.1.2. Ni_3Fe alloys. Ni_3Fe ribbons (width, 1–2 mm; length, about 12 mm; thickness, about 10 μm) were cold rolled and annealed in a pure hydrogen atmosphere, either

(i) at 970 K for 2 h and then successively cooled very slowly from 770 to 760 K (in 3 d), maintained at 760 K for 15 h and slowly cooled from 760 K to room temperature, in order to obtain long-range-ordered alloys or

(ii) at 970 K for 2 h and then quenched (at about 10 K s^{-1}) in order to obtain disordered alloys.

Table 1. Electrical characteristics of the various types of irradiated target.

Target	$\rho_{4.2\,K}$ ($\mu\Omega$ cm)	$\rho_{300\,K}/\rho_{4.2\,K}$
Ordered Cu_3Au	2	3.0
Disordered Cu_3Au	11	1.3
Ordered Ni_3Fe	3.37	3.0
Disordered Ni_3Fe	4.25	3.8
$Fe_{64}Cr_{17}Ni_{19}$	55.2 ± 1.7	1.44
$Fe_{59}Cr_{17}Ni_{24}$	64.4 ± 1.9	1.37
$Fe_9Cr_{18}Ni_{73}$	102.74 ± 0.37	1.02
Amorphous $Fe_{85}B_{15}$	130 ± 10	1.04
and Fe [18]	0.07	143
for comparison		

2.1.3. Austenitic Fe–Cr–Ni alloys. The Fe–Cr–Ni alloys investigated were prepared by melting together weighted quantities of pure (99.997% or higher) iron, pure (99.995% or higher) chromium and pure (99.998% or higher) nickel in an inductive plasma furnace [12]. The obtained concentrations were within 0.08% of the nominal concentrations. Ribbons (width, 1–2 mm; length, about 15 mm; thickness, 10–30 μm) were cold rolled from the ingot, electrolytically etched, annealed for 30 min at 1275 K in a 10^{-4} Pa vacuum and then furnace cooled.

2.1.4. General remarks. Some relevant characteristics of the targets are reported in table 1.

2.2. Irradiation and measurements

The targets consist of stacks of several ribbons of each type of alloy which are piled up perpendicularly to the ion beam (in order to change the ion energy, i.e. the average electronic stopping power, from one sample to another). They were simultaneously irradiated at 4.2 K in a liquid-helium cryostat with 27 MeV/nucleon ^{129}Xe ions delivered by the GANIL accelerator. The incident ions first go through a 2.5 μm thick tantalum sheet that is permanently set in the beam in order to monitor continuously the ion flux and then through a stainless steel window 12.5 μm thick which separates the vacuum of the accelerating tube from the irradiation cryostat. The effective incident ion energy when entering the targets is thus reduced to 3.08 GeV.

The ion flux (homogeneously swept on a 10 cm^2 surface) was always kept lower than 4×10^8 ions $cm^{-2}\,s^{-1}$ in order to limit the heating of the targets during irradiation (the thermocouples located in the irradiated area close to the samples give an average temperature increase of 5–8 K).

Four platinum threads are soldered on each ribbon in order to measure *in situ* the electrical resistance variations of each sample during the irradiation.

Small ribbons (length, about 15 mm; thickness, about 20–30 μm) of two austenitic alloys ($Fe_{64}Cr_{17}Ni_{19}$ and $Fe_9Cr_{18}Ni_{73}$), characterised by high electrical resistivity values, were also irradiated below 90 K with 3.08 GeV xenon ions at a total fluence of

2×10^{13} ions cm^{-2}. Before irradiation, a series of small indentations, at a distance of about 1 mm from one another, were produced with a Vickers microhardness tester (load, 100 g). Their positions were adjusted by moving the mechanical stage of the tester with a micrometer screw. The samples were located in a double-gutter cut in a copper holder. One end of the ribbons was pressed under a clamp, and the other was free. The distances separating two neighbouring indentations are measured with an uncertainty of 2 μm. The relative length changes $\Delta l/l_0$ induced by irradiation were determined by measuring the spacing between the indentations before and after irradiation.

2.3. Interactions of the incident beam with the target

Energetic ions which penetrate in matter lose their energy via

(i) elastic collisions with the target nuclei and
(ii) inelastic collisions with the target electrons.

For gigaelectron volt ions, the latter process is dominant (in our targets the electronic stopping power is typically $(dE/dx)_{elect} \simeq 3$–5 keV $Å^{-1}$), except in the stopping zone of the ions (i.e. the last few microns in which ions have lost most of their energy). In the present experiment, the total thickness of each pile of samples was carefully chosen to be slightly smaller than the calculated ion range [13, 14], so that the ratio of electronic to nuclear stopping powers was always very high $((dE/dx)_{elect}/(dE/dx)_{nucl} \simeq 2000)$.

Elastic collisions produced during low-temperature irradiation of concentrated alloys which exhibit order–disorder phenomena usually lead to the following effects:

(i) In initially chemically disordered alloys, ion irradiation induces displacement cascades. This Frenkel pair creation leads to an increase in the amount of lattice defects in the alloys and thus to an increase in their electrical resistivity:

$$\Delta\rho_{\text{disordered alloys}} = \Delta\rho_{\text{displacement}}.$$

(ii) In initially chemically ordered alloys, a term which accounts for the replacements occurring during the displacement phase (especially during focused collisions along dense atomic rows) must be added to the displacement contribution. There is thus a supplementary resistivity term related to the formation of anti-site defects:

$$\Delta\rho_{\text{ordered alloys}} = \Delta\rho_{\text{displacement}} + \Delta\rho_{\text{AS}}.$$

(iii) At sufficiently high temperatures and for some alloys, irradiation can induce reordering phenomena [15].

It was shown in [4] that in Cu_3Au, at irradiation temperatures ($T \simeq 20$ K) sufficiently low that thermal migration of point defects does not occur, there is no ordering during irradiation. For Ni_3Fe alloys no quantitative information on order–disorder phenomena under irradiation is available to our knowledge.

2.4. Displacements per atom calculations

This section presents calculations of the percentage of target atoms displaced during irradiation with high-energy heavy ions. Elastic collisions between the incident ions and the target atoms are only considered with the assumption that the defect production mechanism is not modified by high electronic energy loss occurring simultaneously.

The integral equations in [16] governing radiation damage have been slightly modified [17, 18] in order to calculate directly the number of displaced atoms during an irradiation of polyatomic targets with gigaelectron volt ions, taking into account that

(i) the various types of target atom have different threshold displacement energies and

(ii) a displacement cascade initiated by an atom of a given type induces displacements of the different types of target atom.

In [4] the threshold displacement energies of copper and gold in an ordered Cu_3Au alloy irradiated with megaelectron volt electrons were determined:

$$E_d^{Cu} = 22\,eV$$

$$E_d^{Au} = 18\,eV.$$

Using these threshold values, the electronic stopping power at low energies [18] and the electronic stopping power at high energies [14], the numbers of displaced atoms of each type including the atomic displacements and replacements (i.e. anti-structure defects) can be calculated in an ordered Cu_3Au alloy. It should, however, be mentioned that anti-structure defects resulting from focused collision sequences cannot be taken into account in such an analytical calculation. The results are nevertheless reliable as long as they are used only for the purpose of comparing defect production in various gigaelectron volt ion irradiations.

For the initially disordered Cu_3Au alloy, there is no chemical disorder term, so that the numbers of displaced atoms can be calculated in an average target.

In Ni_3Fe alloys and in austenites, in which the threshold displacement energies of the various types of atom were not determined, we used a unique threshold value (E_d = 20 eV) to calculate the concentration C_{th} of defects expected at an irradiation fluence Φt.

On comparison of these theoretical predictions with experimental results, it is then possible to determine whether the defect production mechanism is modified when the incident ions strongly excite the target electrons.

3. Results and discussion

3.1. Dimensional measurements

In the two austenitic alloys which were studied, the irradiation did not produce relative length changes larger than 1.5×10^{-3} (measured on a length of 7–9 mm). This result should be compared with the huge length variations ($\Delta l/l > 10^{-2}$) obtained in amorphous $Fe_{85}B_{15}$ irradiated at 77 K with 3 GeV xenon at a dose of 2×10^{13} ions cm^{-2} [1]. It is worth noting that amorphous $Fe_{85}B_{15}$ has a low-temperature electrical resistivity of 130 $\mu\Omega$ cm (table 1), which is very close to that of one of the austenites. We can thus conclude that the radiation-induced growth observed in amorphous alloys appears to be specific to the amorphous structure and is not simply related to their high electrical resitivity.

3.2. Electrical resistivity

For each type of alloy, and for each ribbon of the piled-up targets, the average electronic energy loss of the xenon ions into the sample (from 3 to 5 keV $Å^{-1}$) was calculated

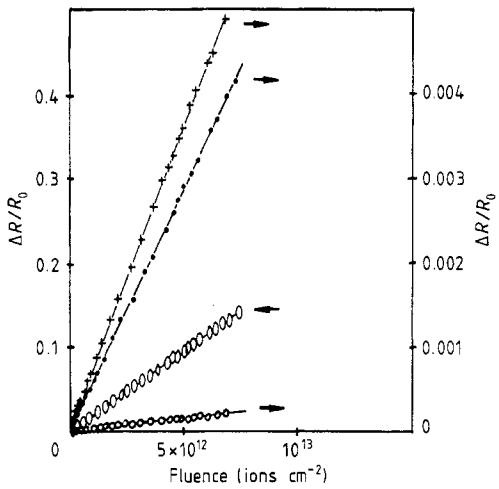

Figure 1. Typical relative electrical resistance variation $\Delta R/R_0$ versus ion fluence for various alloys irradiated at liquid-helium temperature with high-energy Xe ions (the average electronic energy losses are given in parentheses: +, ordered Ni_3Fe (3.05 keV $Å^{-1}$); ●, disordered Ni_3Fe (4.06 keV $Å^{-1}$); 0, ordered Cu_3Au (4.64 keV $Å^{-1}$); ○, austenite (2.9 keV $Å^{-1}$).

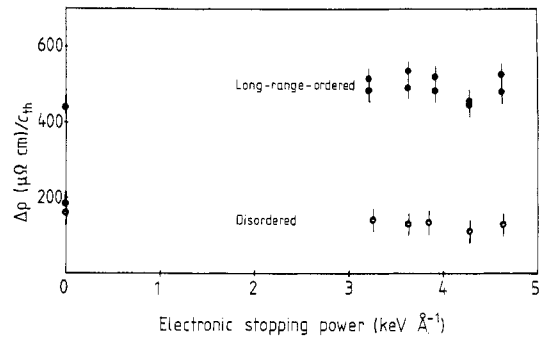

Figure 2. Ratio of the initial resistivity increase to the theoretical concentration of defects created by elastic collisions versus the average ion electronic stopping power for Cu_3Au alloys irradiated at a low temperature with high-energy Xe ions and with megaelectronvolt electrons. Note that two data were sometimes recorded as the same $(dE/dx)_{elect}$ value (repeated points in the figure), indicating good reproducibility of the results.

and the initial electrical resistance increase ΔR induced by irradiation at a fluence Φt measured *in situ* at 10 K (figure 1). Since no noticeable dimensional change of the irradiated ribbons is evidenced, the electrical resistivity variation $\Delta\rho$ is proportional to ΔR. On the assumption that the value of $\Delta\rho$ is proportional to the effective defect concentration introduced during irradiation, $r = \Delta\rho/C_{th}$ is then proportional to the ratio of effective to calculated radiation-induced defect concentrations. This ratio is plotted as a function of the average electronic energy loss of the ions in the various types of target investigated (figures 2 and 3).

We also plotted in figure 2 the ratio r obtained during 20 K irradiations of ordered and disordered Cu_3Au alloys with 1.5–2.5 MeV electrons [4, 5] ($(dE/dx)_{elect} \simeq 0.1$ eV $Å^{-1}$). The results show that the ratio r is independent of the amount of electronic energy loss inside the sample up to $(dE/dx)_{elect} \simeq 4.7$ keV $Å^{-1}$, although the comparison between the defect concentration calculated following electron and ion irradiations is not fully reliable (see section 2.4). On the other hand, the results relative to xenon irradiations

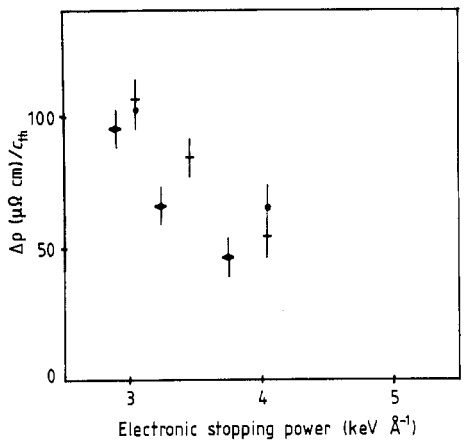

Figure 3. As figure 2, but for Ni-based alloys irradiated with high-energy Xe ions: ●, ordered Ni_3Fe; +, disordered Ni_3Fe; ◆, $Fe_{59}Cr_{17}Ni_{24}$ austenite.

of ordered and disordered Ni_3Fe and $Fe_{59}Cr_{17}Ni_{24}$ austenite clearly indicate (figure 3) a decrease in the observed defect production rate as the electronic stopping power of the ions increases. Let us recall that modifications of defect production [16, 19] and defect stability [20] in pure iron and nickel targets irradiated at a low temperature with high-energy ions have been already reported.

At the end of the irradiation, the ordered and disordered Ni_3Fe samples were submitted to 10 min isochronal annealing from 60 K to room temperature. Figure 4 shows typical recovery curves relative to different average electronic stopping powers of the xenon ions in the samples. The following points should be noted:

(i) There is no marked annealing stage. After a small recovery up to 120 K, a continuous resistivity decrease is observed up to 300 K.

(ii) For all samples, the electrical resistivity measured at 10 K after annealing up to room temperature is smaller than that measured before irradiation. This is certainly a consequence of reordering effects which result from the thermal migration of radiation-induced point defects.

(iii) For both ordered and disordered Ni_3Fe samples, the annealing effect becomes larger as the average amount of energy lost by the incoming ions in inelastic interactions decreases. A modification of the annealing curve is mainly observed in the low-temperature range, i.e. in the region relative to the annihilation of isolated irradiation defects. At higher temperatures, the recovery curves relative to different electronic stopping powers remain parallel.

Similar behaviours were previously observed in pure iron [16] and nickel [19], for which the recovery curves indicate that electronic excitation mainly induces a decrease in the number of remaining isolated irradiation defects.

4. Conclusion

The purpose of this paper was to study the effect on elastic-collision-induced damage production of high electronic excitation ($(dE/dx)_{elect} \simeq 3$–5 keV Å^{-1}) produced during

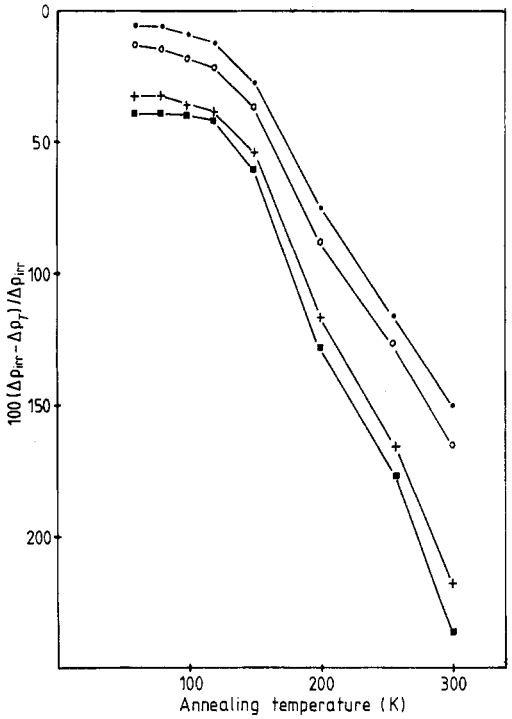

Figure 4. Percentage of resistivity recovery versus temperature during isochronal annealing of ordered (○, ●) and disordered (■, +) Ni_3Fe alloys irradiated at liquid-helium temperature with high-energy Xe ions. The average electronic energy losses $(dE/dx)_{elect}$ inside each ribbon are as follows: ○, ■, 3.05 keV Å^{-1}; ●, +, 4.06 keV Å^{-1}.

low-temperature high-energy heavy-ion irradiation. The systems investigated were metallic alloys presenting a broad range of electronic and structural properties. The main results are the following.

(i) Inelastic collisions do not modify appreciably the damage production in both ordered and disordered Cu_3Au alloys.

(ii) In the austenite and Ni_3Fe alloys, a decrease in the defect production efficiency is evidenced as the ion electronic stopping power increases. More precisely, this can be attributed to the recombination of part of the close Frenkel pairs induced in nuclear collisions.

When it occurs, the reduction in the damage production efficiency as the amount of electronic energy loss increases might be related to some momentum transfer mechanisms between the excited electrons and the target atoms leading to subthreshold events, local heating above stage I temperature, collective effects, etc. In [21] it was shown that, in d- and f-band metals, several factors contribute to increasing the ability of the electronic system to couple to the lattice atoms. According to this idea, the higher densities of d states at the Fermi level in iron and nickel-based alloys compared with copper-based alloys could explain our observations: Cu [19] and Cu_3Au alloys are not sensitive to high electronic excitation levels, whereas Fe [16, 20], Ni [19], Ni_3Fe and austenite are.

Finally, it is important to mention that more drastic effects could well occur at higher electronic stopping powers, i.e. following irradiation with heavier (e.g. U) irradiating ions.

Acknowledgments

The authors greatly acknowledge Dr Y Calvayrac (Centre d'Etudes de Chimie Métallurgique, Vitry) who prepared the Ni_3Fe alloys. The irradiations were performed at the National Laboratory GANIL, Caen (France) with the technical assistance of the Centre Interdisciplinaire de Recherche avec les Ions Lourds.

References

[1] Audouard A, Balanzat E, Fuchs G, Jousset J C, Lesueur D and Thomé L 1987 *Europhys. Lett.* **3** 327; 1988 *Europhys. Lett.* **5** 241
[2] Audouard A, Balanzat E, Jousset J C, Fuchs G, Lesueur D and Thomé L 1990 *Phil. Mag.* at press
[3] Klaumünzer S, Ming-Dong Hou and Schumacher G 1986 *Phys. Rev. Lett.* **57** 850
[4] Alamo A 1983 *Commissariat à l'Energie Atomique* R-5231
[5] Alamo A, Desarmot G and Dirand M 1982 *Radiat. Eff.* **59** 137
[6] Jenkins M L and Wilkens M 1976 *Phil. Mag.* **34** 1155
[7] Dunlop A, Lesueur D, Morillo J and Thomé L 1990 to be published
[8] Sakairi H, Yagi E, Komaya A and Hasiguti R R 1981 *J. Phys. Soc. Japan* **50** 3023
[9] Dimitrov C, Da Cunha Belo M and Dimitrov O 1980 *J. Phys. F: Met. Phys.* **10** 1653
[10] Johansson C H and Linde J O 1925 *Ann. Phys., Lpz.* **78** 439
[11] Calvayrac Y and Fayard M 1973 *Phys. Status Solidi* a **17** 407
[12] Dimitrov C, Tenti M and Dimitrov O 1981 *J. Phys. F: Met. Phys.* **11** 753
[13] Hubert F, Fleury A, Bimbot R and Gardes D 1980 *Ann. Phys., Paris* **5** 1
[14] Ziegler J F 1980 *Stopping and Ranges of Ions in Matter* vol 5 (Oxford: Pergamon)
[15] Schulson E M 1978 *J. Nucl. Mater.* **83** 239
[16] Lindhard J, Nielsen V, Scharff M and Thomsen P V 1963 *K. Dan. Vidensk. Selsk. Mat. Fys. Medd.* **33**
[17] Dunlop A, Lesueur D and Dural J 1989 *Nucl. Instrum. Methods* B **42** 182
[18] Alberman A and Lesueur D 1989 *Proc. 6th Symp. ASTM–Euratom Reactor Dosimetry* ed H Farrar IV and E P Lippincott
[19] Iwase A, Sasaki S, Iwata T and Nihira T 1986 *Phys. Rev. Lett.* **58** 2450
[20] Dunlop A, Lesueur D, Jaskierowicz G and Schildknecht J 1989 *Nucl. Instr. Methods* B **36** 412
[21] Seitz F and Koehler J S 1956 *Solid State Phys.* **2** 305 (New York: Academic)